*electrochem*

MDPI

*Article*

# Pseudospherical Bismuth Oxychloride-Modified Carbon Paste Electrode for the Determination of Quinine in Beverages

**Tijana Mutić [1,*], Vesna Stanković [1], Miloš Ognjanović [2], Vladimir B. Nikolić [3], Guanyue Gao [4,5], Neso Sojic [6] and Dalibor Stanković [3]**

[1] Institute of Chemistry, Technology and Metallurgy, National Institute of the Republic of Serbia, University of Belgrade, Studentski trg 12-16, 11000 Belgrade, Serbia; vesna.stankovic@ihtm.bg.ac.rs
[2] Vinča Institute of Nuclear Sciences, University of Belgrade, Mike Petrovića Alasa 12–14, 11000 Belgrade, Serbia; miloso@vin.bg.ac.rs
[3] Faculty of Chemistry, University of Belgrade, Studentski trg 12–16, 11000 Belgrade, Serbia; nikolicv@chem.bg.ac.rs (V.B.N.); dalibors@chem.bg.ac.rs (D.S.)
[4] Key Laboratory of Photochemical Conversion and Optoelectronic Materials, Technical Institute of Physics and Chemistry, Chinese Academy of Sciences, Beijing 100190, China; gaoguanyue@mail.ipc.ac.cn
[5] University of Chinese Academy of Sciences, Beijing 100049, China
[6] Institut des Sciences Moléculaires, University of Bordeaux, CNRS, Bordeaux INP, UMR 5255, 33607 Pessac, France; sojic@u-bordeaux.fr
* Correspondence: tijana.mutic@ihtm.bg.ac.rs

**Abstract:** The extensive use of the alkaloid quinine (QN) in the cosmetic and food industries has induced major concerns relating to its impact on human health, considering its potential toxicity. Therefore, developing sensitive and selective electrochemical sensors is crucial for monitoring QN in environmental, food, and pharmaceutical samples. To respond to this need, a surfactant-supported green synthesis approach, based on a straightforward, organic solvent-free hydrothermal method was employed to synthesize highly crystalline pseudospherical bismuth oxychloride (BiOCl) nanoparticles. This material was used for the enrichment of carbon paste electrodes and its further utilization for the detection and quantification of quinine. They have superior electrocatalytic performance, due to their size and morphology, and facilitate the interactions of the target with the electrode surface. Under optimal operating conditions, differential pulse voltammetry demonstrated a remarkable feature: a broad linear working range of 10 to 140 μM, a detection limit of 0.14 μM, and a high sensitivity of 1.995 μA $\mu M^{-1}$ $cm^{-2}$. The suggested method's satisfactory sensitivity, along with its good stability, repeatability, and reproducibility, strongly point to a possible use for identifying quinine in real samples.

**Keywords:** electrochemical sensor; carbon paste electrode; nanomaterials; malaria; alkaloids



**Citation:** Mutić, T.; Stanković, V.; Ognjanović, M.; Nikolić, V.B.; Gao, G.; Sojic, N.; Stanković, D. Pseudospherical Bismuth Oxychloride-Modified Carbon Paste Electrode for the Determination of Quinine in Beverages. *Electrochem* **2024**, *5*, 407–420. https://doi.org/10.3390/electrochem5040027

Academic Editor: Masato Sone

Received: 12 September 2024
Revised: 7 October 2024
Accepted: 12 October 2024
Published: 15 October 2024



## 1. Introduction

One of the deadliest diseases in the world's history is malaria. According to the World Health Organization (WHO), 241 million cases of infection and 627 thousand deaths in 85 malaria-endemic countries were reported in 2021 [1]. The most cases of malaria were reported in the African Region, 95%, led by Nigeria (27%), the Democratic Republic of the Congo (12%), Uganda (5%), Mozambique (4%), Angola (3.4%), and Burkina Faso (3.4%) [1].

Quinine (QN), namely, (R)-[(2S,4S,5R)-5-ethenyl-1-azabicyclo[2.2.2]octan-2-yl]-(6-methoxyquinolin-4-yl)-methanol, is a white, bitter-tasting crystalline alkaloid isolated from the bark of the cinchona tree (*Cinchona calisaya*) [2,3]. For the last 300 years, quinine has been used as a very effective medicine in the fight against malaria, caused by the parasite *Plasmodium falciparum* [4,5], which is resistant to other antimalarials such as chloroquine, quinacrine, and primaquine. Quinine exhibits antibacterial, antiseptic, local anesthetic, and analgesic effects and acts as a cardiovascular stimulant. In addition to malaria, the drug is used in the treatment of muscle spasms and in the case of resistance to other drugs during

chemotherapy. In addition to medical use, quinine is also used in the cosmetic industry, as a tonic, antiseptic, and lotion [6], and in the food industry, especially in the beverage industry, where it is added to achieve a bitter taste in soft drinks, most often tonic water or cocktails containing tonic [7,8]. In addition to all the above properties, quinine can also have a potentially toxic effect and cause several side effects such as nausea, blurred vision, diarrhea, stomach pain, headache, fever, and asthma [9].

The attractiveness of nanomaterials in electroanalytical chemistry has drawn the interest of many research groups to investigate in detail the influence of the material's morphological characteristics on its electrocatalytic capabilities [10–14]. A large number of different metals participate in the formation of these nanoparticles. Materials based on bismuth offer great potential in electrocatalysis. So far, a large number of bismuth-based nanomaterials of various structures have been reported that have shown excellent electrocatalytic properties [15–17].

Considering the potentially toxic effect of quinine on human health, several analytical techniques have been developed for its determination in biological, pharmaceutical, and food samples. Analytical techniques used for the determination of quinine are High-Performance Liquid Chromatography (HPLC) [18,19], Chemiluminescence [20,21], Gas Chromatography–Mass Spectrometry (GC-MS) [22,23], and Capillary Electrophoresis (CE) [24,25]. All the mentioned methods, although effective, are costly and require a lot of time and consumption of toxic reagents. Therefore, it is essential to develop a fast, simple, cheap, and effective method for the determination of quinine content. Electrochemical methods offer several advantages over the mentioned methods, which are reflected in the simplicity of operation, low prices, sensitivity, and the speed of analysis. Furthermore, electrochemical systems can be converted into portable systems for in vivo and in vitro analysis [26]. The application of the modified electrode as a working electrode in electrochemical systems is useful for trace-level analysis. Modified electrodes reduce the potential of the redox process and increase the sensitivity of the analysis of electroactive compounds [27]. In addition to the mentioned conventional techniques, electrochemical methods were employed for quinine detection and quantification in a few works. Electrodes previously used in these works are glassy carbon electrode [3], hanging mercury drop electrode [6], pencil-graphite electrodes [28,29], and boron-doped diamond electrode [30].

In this work, bismuth oxychloride nanoparticles were synthesized by a chemical hydrothermal procedure and used for the modification of carbon paste electrode for detection and quantification of quinine. Considering the excellent electrocatalytic properties of bismuth-based materials, synthesized BiOCl was thoroughly investigated morphologically and electrochemically. The developed method was utilized for a real sample study of beverage drinks under optimized parameters, examining its potential application in everyday routine analysis.

## 2. Materials and Methods

### *2.1. Chemicals and Reagents*

Bismuth trichloride monohydrate ($BiCl_3 \times H_2O$; 99.99%), polyethylene glycol 400 (PEG 400; for synthesis), hydrochloric acid (HCl; puriss. p.a), sodium hydroxide (NaOH; ≥98%), Quinine (Mr = 324.4; ≥98.0%), and all other chemicals were of analytical grade and purchased from Sigma-Aldrich (St. Louis, Missouri, United States). Britton–Robinson buffer solution (BRBS) was prepared by mixing 0.04 M of each boric acid, phosphoric acid, and acetic acid; the pH value was adjusted using 0.1 M sodium hydroxide solution. BRBS was used as a supporting electrolyte in electrochemical measurements. Double-distilled water (DD water) was used for the preparation of solutions. For voltammetric measurements, 5 mM potassium hexacyanoferrate (III) ($K_3[Fe(CN)_6]$) and potassium hexacyanoferrate (II) trihydrate ($K_4[Fe(CN)_6]\cdot 3H_2O$) in 0.1 M KCl solution was used. Quinine solution was prepared by dissolving a stochiometric amount of quinine in sulfuric acid.

### *2.2. Instrumentation*

The crystal structure of bismuth oxychloride nanoparticles was determined using X-ray Powder Diffraction (XRD) data measured on dried powders in a high-resolution SmartLab® diffractometer (Rigaku, Japan), equipped with Cu K$\alpha$ radiation source ($\lambda$ = 1.5406 Å) under a voltage of 40 kV and a 30 mA current. The patterns were collected within the 10–70° 2$\theta$ range at a scan rate of 1°/min and 0.02° step size. Transmission electron microscope Jeol JEM-2100F (JEOL, Tokyo, Japan) and scanning electron microscope Jeol JSM-7001F (JEOL, Tokyo, Japan) were used to scrutinize the morphological properties of the material. The accelerating voltage of the electron gun was set to the 20 kV required for quantitative EDX analysis.

All electrochemical measurements were performed using a PalmSens4 analyzer (Houten, Utrecht, The Netherlands) with PSTrace voltammetry software (Version 5.8) at room temperature. A conventional standard three-electrode system was used with an unmodified and a modified carbon paste electrode as a working electrode, an Ag/AgCl electrode as a reference electrode, and platinum wire as a counter electrode. A DPV method was developed for QN quantification and measurements were recorded at amplitude 25 mV with both pulse width and period 0.2 s, in a potential range from 0.5 to 1.5 V.

The developed method was validated using the standard UV–Vis method. A Thermo Scientific Evolution 201/220 UV–Visible Spectrophotometer with a 10 mm quartz cell was used for all absorption measurements.

### *2.3. Methods*

The synthesized nanomaterial was characterized morphologically using X-ray Diffraction (XRD), Scanning Electron Microscopy (SEM), and Transmission Electron Microscopy (TEM).

The electrochemical properties of the BiOCl-modified carbon paste electrode were examined using Cyclic Voltammetry (CV), Electrochemical Impedance Spectroscopy (EIS), Square-Wave Voltammetry (SWV), and Differential Pulse Voltammetry (DPV). Method validation was performed using UV–Visible Spectrophotometry (UV–Vis).

### *2.4. Synthesis of BiOCl*

Bismuth oxychloride (BiOCl) nanoparticles were synthesized by a chemical hydrothermal method following a modified procedure from the literature [31]. This synthesis method involved dispersing a stoichiometric amount of $BiCl_3$*$H_2O$ (0.2 M) in 100 mL of DD water and 2 mL of HCl solution with continuous magnetic stirring. To obtain a uniform dispersion, PEG 400 and a 1 M NaOH solution were thereafter gradually added to the suspension while being stirred for two hours at room temperature. The obtained residue was then transferred into a hydrothermal autoclave and treated at 180 °C for 12 h. The resultant product was washed with ethanol and DD water several times to remove the unreacted species, and excess solvents were dried in a vacuum oven overnight at 80 °C. Finally, the collected samples were followed up by thermal treatment at 450 °C for 3 h.

### *2.5. Preparation of Unmodified and Modified Carbon Paste Electrodes*

All of the carbon paste electrodes were prepared by mechanically mixing carbon powder with paraffin oil for approximately 30 min. An unmodified electrode was prepared by mixing 80 mg of carbon powder with 20 µL paraffin oil until a homogenous paste was achieved. Modified electrodes were prepared by adding 2 mg (2%), 4 mg (5%), 6 mg (7%), and 8 mg (10%) of synthesized material to the carbon powder (to a total mass of 80 mg) and paraffin oil. Prepared electrodes were stored in a fridge for at least 24 h before measurements. A homemade Teflon electrode body with an inner diameter of 2 mm was loaded with the obtained paste and smoothed on a paper towel to produce a uniform surface, before and between all measurements.

## 3. Results and Discussion

### *3.1. Morphological Characterization of Synthesized Material*

TEM analysis revealed pseudospherical nanoparticles with an average size of (9 ± 2) nm (Figure 1A,B). Particles are uniform and partially agglomerated with clearly visible crystal planes on HRTEM micrographs, suggesting the crystalline nature of the sample. The uniform spherical structure of the nanoparticles can be attributed to the influence of the PEG surfactant present during the synthesis of the material since similar structures were reported by Zhang et al. and Li et al. [32,33]. The XRD pattern of the BiOCl sample is shown in Figure 1C. The prepared BiOCl was crystallized into a standard tetragonal structure (PDF card #90082426). The intense and sharp diffraction peaks suggested that the as-synthesized product was well-crystallized. There are no other impurity peaks observed in the patterns. The average crystallite size was assessed using the Scherrer formula of the most intensive diffraction maximums and was found to be 8 ± 2 nm. The similar sizes obtained by TEM and XRD suggest that nanoparticles are formed out of single crystallite. FE-SEM elemental mapping (Figure 1D,E) revealed the presence of Bi, Cl, and O atoms in the whole mapped area, confirming the successful formation of bismoclite nanoparticles throughout the whole sample.

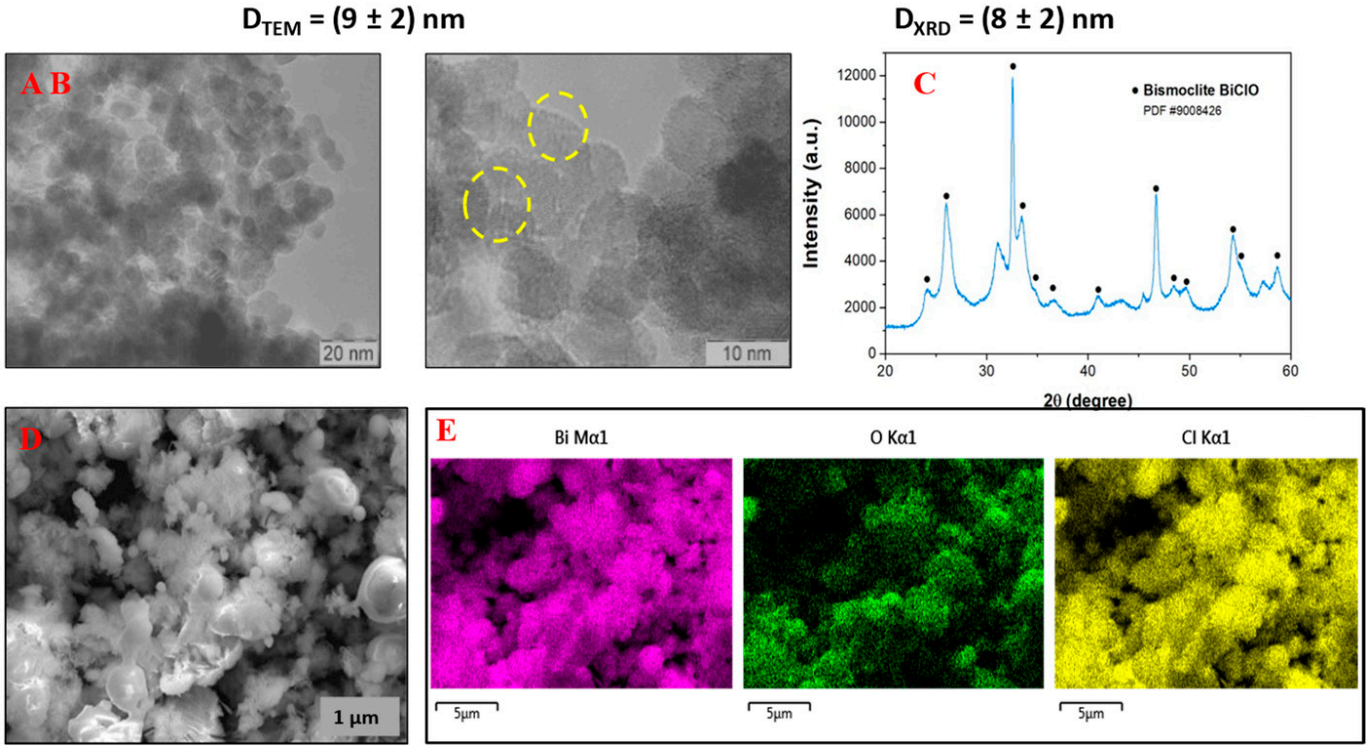


**Figure 1.** (**A**,**B**) TEM image of the prepared sample; (**C**) XRD pattern of the BiOCl sample; (**D**,**E**) FE-SEM and elemental mapping for BiOCl.

### *3.2. Electrochemical Characterization of Prepared Electrode*

EIS was used to investigate the electrolyte–electrode charge-transfer mechanism over both modified and unmodified electrodes since it is a popular analytical electrochemical technique for the fast, accurate, and non-invasive examination of conductive materials. EIS was performed over electrodes in a standard solution of 5 mM $K_3[Fe(CN)_6]$ and $K_4[Fe(CN)_6]$, containing 0.1 M KCl supporting electrolyte. Nyquist plots (EIS spectra) are composed of two parts: a semicircular high-frequency region, whose diameter represents a quantitative value of resistance to charge transfer, and a linear low-frequency area, which depends on mass transfer. The semicircle's diameter is very small for materials that have kinetically quick charge transport [34]. As shown in Figure 2A, a 5% BiOCl-modified carbon paste electrode has a lower value of resistance (512 Ω) than a bare carbon paste electrode

(5159 Ω) and 2% (1987 Ω), 7% (1904 Ω), and 10% (1657 Ω) BiOCl-modified CPEs, meaning that the active surface area of the modified electrode is higher than the bare carbon paste electrode. The credit for this can be attributed to the use of PEG 400, which was effective for the control of the size and shape of nanoparticles. Indeed, it affected the size (9 ± 2 nm) and spherical morphology of the final obtained nanoparticles. In addition, the superior characteristics and advantages of this material, such as non-toxicity, non-immunogenicity, and high water solubility, support and recommend the use of this material in various applications.

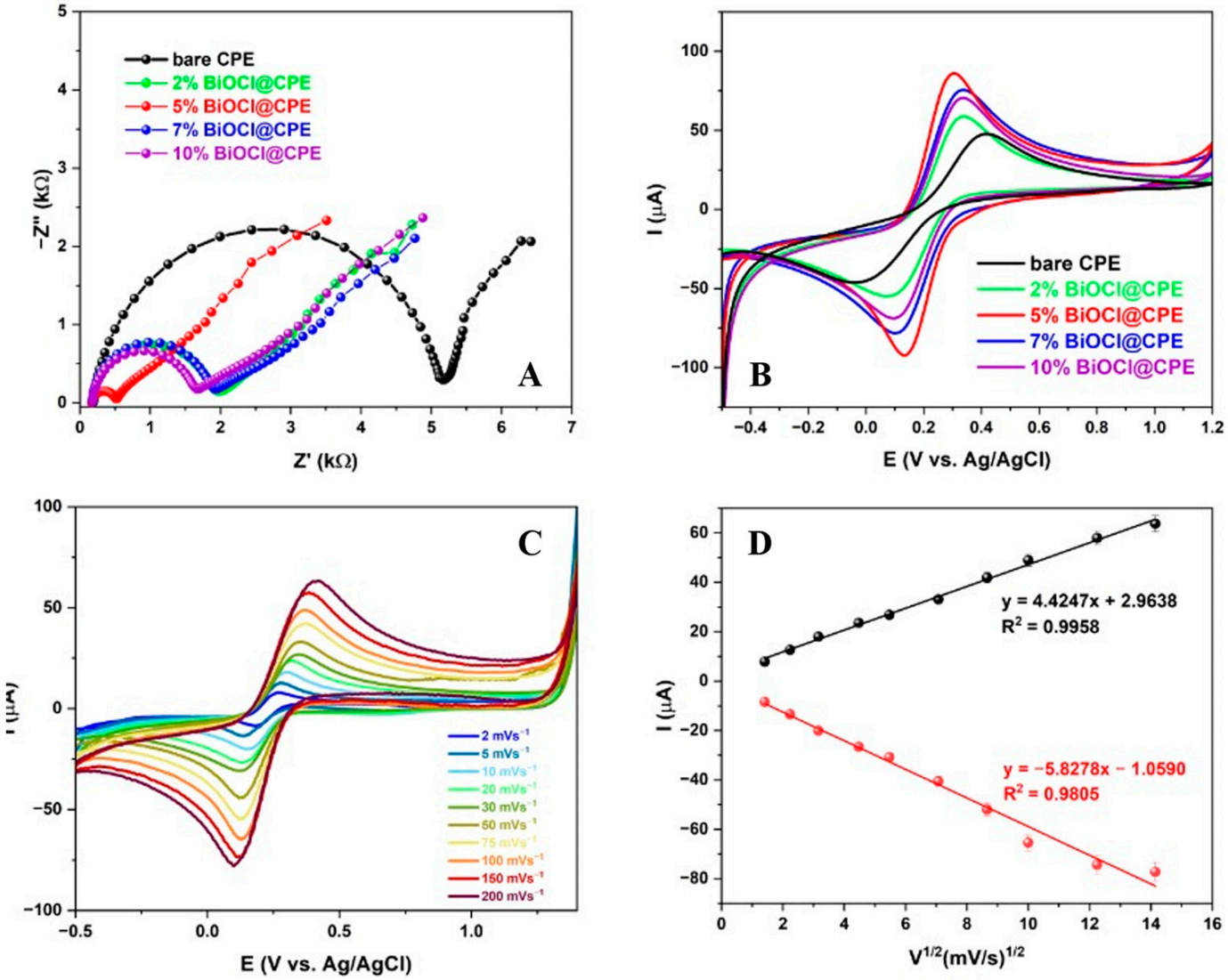


**Figure 2.** (**A**) EIS spectra (Nyquist plot) of 5 mM $[Fe(CN)_6]^{3-/4-}$ and 0.1 M KCl of bare and BiOCl-modified CPEs at amplitude 5 mV, in a range from $10^{-2}$ to $10^5$ Hz; (**B**) Cyclic voltammograms of 5 mM $[Fe(CN)_6]^{3-/4-}$ and 0.1 M KCl of bare and BiOCl-modified CPEs at 50 $mVs^{-1}$; (**C**) Cyclic voltammogram of 5 mM $[Fe(CN)_6]^{3-/4-}$ and 0.1 M KCl of BiOCl-modified CPEs at different scan rates in the range from 2 to 200 $mVs^{-1}$; (**D**) Dependence of redox peak current on the square root of the scan rate.

The BiOCl-modified and unmodified carbon paste electrodes were tested by CV measurements in the same solution containing the $[Fe(CN)_6]^{3-}/[Fe(CN)_6]^{4-}$ redox couple. The voltammograms show the electron transfer behavior of electrodes, and the 5% modified electrode displays well-defined redox peaks at a 50 mV $s^{-1}$ scan rate in both forward and backward scans in the potential range from −0.5 V to 1.2 V (Figure 2B). The increase in

peak currents as well as the decrease in the peak-to-peak separation values, as the two most-important parameters, strongly suggest that the electrode has an excellent electron transfer process and higher electrochemical activity, compared to the unmodified carbon paste electrode. Since CV can reveal the mechanism of the reaction, CV measurements were performed in the same solution, in the same electrochemical window, but with different scan rates (2 $mVs^{-1}$ to 200 $mVs^{-1}$), as shown in Figure 2C. Increasing the scan rate also increases the anodic and cathodic peak currents. Analysis showed that the correlation between the currents of the redox peak and the square root of the scan rate is linear, as evidenced in Figure 2D, with equations y = 4.4247x + 2.9638 with a linear regression coefficient $R^2$ 0.99 for oxidation and y = −5.8278x − 1.0590 with an $R^2$ of 0.98 for reduction. These results and this linear correlation confirmed that the mechanism of this redox process is diffusion-controlled. The electrochemically active surface area was calculated using the Randles–Sevcik equation [35]:

$$Ip = 2.69 \times 10^5 \times n^{\frac{3}{2}} \times A \times C \times \sqrt{D} \times V$$

where Ip is the peak current (A), n is the number of electrons in the redox reaction, A is the electroactive surface area ($cm^2$), D is the diffusion coefficient (D = 6 × $10^{-6}$ $cm^2/s$), C is the concentration of the reaction species in the electrolyte ($mol/cm^3$), and V is the scan rate ($Vs^{-1}$). The calculated surface area for the bare carbon paste electrode was 0.205 $mm^2$, compared to 2, 5, 7, and 10% BiOCl-modified CPEs, whose calculated values were 0.254 $mm^2$, 0.371 $mm^2$, 0.324 $mm^2$, and 0.305 $mm^2$, respectively.

### *3.3. Electrochemistry of QN and Method Development*

Data on the capacity and size of the electrode material's active surface, as well as the kinetics of the reaction on the electrode, can be obtained using CV. The voltammetric signals of quinine solution in BRBS at pH 6 were recorded using unmodified and modified carbon paste electrodes with varying percentages of modification. Cyclic voltammograms, shown in Figure 3A, were obtained at a scan rate of 50 $mVs^{-1}$ by recording a 100 µM QN solution in BRBS pH 6 with an electrode modified with 2, 5, 7, and 10% of the BiOCl material. All the tested electrodes provide resolved and well-defined oxidation peaks for QN at the potential of around 0.95 V. However, modified electrodes show an increased peak current, which is shown in the bar diagram (Figure 3B), indicating the promotion of the interaction between the electrode surfaces and the tested analyte. This enhancement starts to decrease for amounts of the modifier higher than 7 wt.%. These results suggest that catalysis loading is an important part of sensor development. Above 7 wt.% loading of BiOCl, the catalyst particles may begin to aggregate. This reduces the exposed catalyst surface area and limits electrolyte access to the active sites. This is observed from the data that we obtained for the BiOCl material with a high catalyst content of 10 wt.%. Furthermore, electrical conductivity through the electrode may be impeded by the high content of the aggregated catalyst particles, which was observed from CV data. Thus, the electrode exhibiting the highest peak current value, with a 5% modifier, was chosen for additional investigation. Electrodes with less than 2% modifier were not tested because the results would not be meaningful due to the inability to homogeneously mix small amounts of material into the carbon paste.

Using a 5% modifier electrode for CV recording, the pH value of the supporting electrolyte was optimized. The CVs of freshly prepared 100 µM QN solution were recorded at a scan rate of 50 $mVs^{-1}$ in the pH range of BRBS supporting electrolyte from 2 to 10. The results are displayed in Figure 3C. There is no discernible QN signal when the pH of the solution is below 5. The CV shows that there is a significant shifting in the peaks towards lower values of the oxidation peak potential as the supporting electrolyte's pH increases. This shift has a clear dependence in the range of pH values of the supporting electrolyte from 5 to 10, and this dependence can be expressed through a linear curve whose corresponding equation is y = −0.054x + 1.406 (Figure 3D). The slope of this curve has a value of 54 mV/pH, indicating that the same number of protons and electrons are involved

in the redox reaction on the surface of the electrode, according to the following equation: Ep = (0.059 m/n)pH + b [36]. The number of transferred electrons in this redox reaction was calculated using the following equation: $Ep - Ep_{1/2} = 47.7\ mV/\alpha n$ [37], where Ep and $Ep_{1/2}$ represent peak potential and peak potential at half-height, and $\alpha$ is 0.5. The calculated number of electrons is 1.17, which is close to 1. Following that, the reaction mechanism was proposed and presented in Scheme 1. Looking at the literature, similar behavior was recently reported by Dushna and co-workers, who reported that the redox reaction of quinine is controlled by one electron and one proton [30]. However, to obtain more detailed data, and to be able to assume reactions at the interface, additional research should be carried out. It is noteworthy that, at higher pH values (9 and 10), the presence of a reduction peak of weak but noticeable intensity was observed. Similar behavior was reported by other authors at this pH as well as in highly acidic solutions [27,28,38,39].

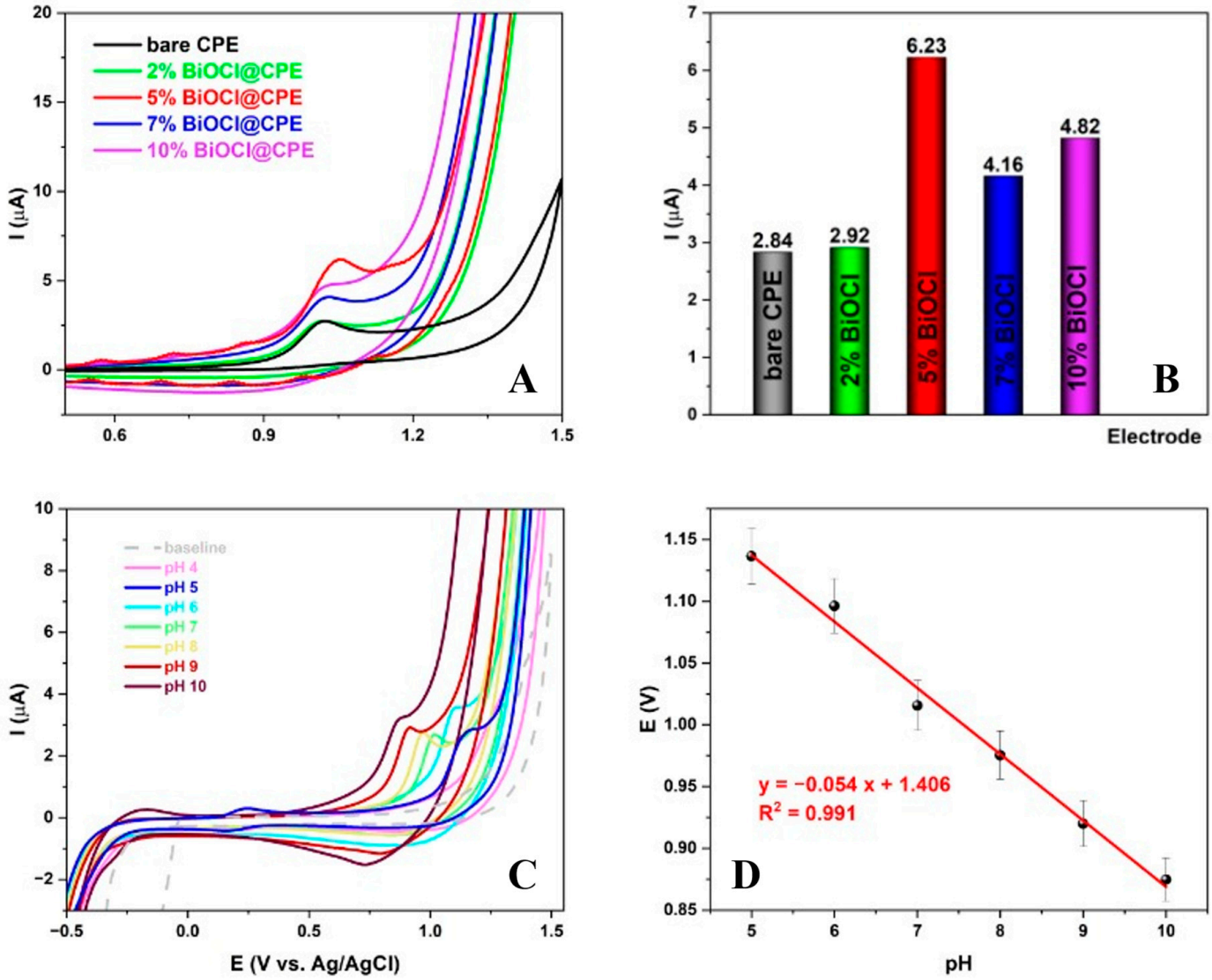


**Figure 3.** (**A**) Electrochemical behavior of QN over bare and differently modified (2, 5, 7, 10%) CPEs at a potential range from −0.5 to 1.5 V in BRBS at 50 $mVs^{-1}$; (**B**) Corresponding bar diagram of the electrochemical behavior of QN over CPEs; (**C**) Cyclic voltammograms of 100 µM QN using 5% BiOCl-modified CPE in BRBS at different pH values in the range from 4 to 10 at 50 $mVs^{-1}$; (**D**) Dependence of the potential of the anodic peak current on pH.

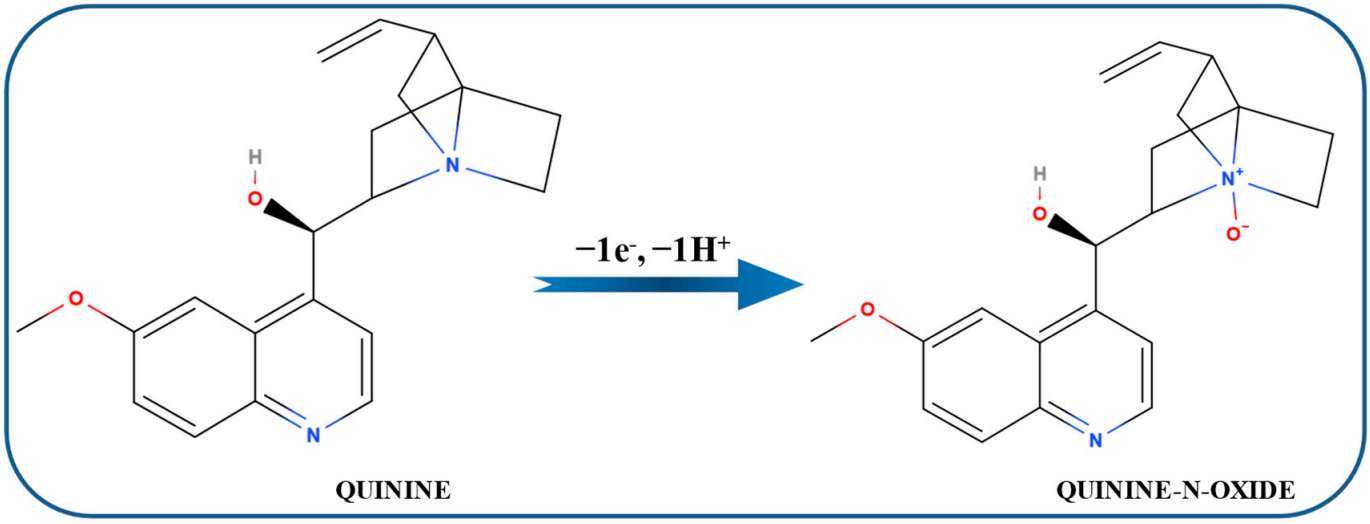


**Scheme 1.** The proposed mechanism of QN redox reaction over the developed BiOCl@CPE sensor.

Since the peak with the highest current value is obtained at pH 6, it was selected as the optimal value for additional testing. Subsequently, CVs were recorded in the BRBS at pH 6 (as was chosen), with scan rates varying from 2 $mVs^{-1}$ to 200 $mVs^{-1}$ (Figure 4A). The graph shows that an increase in the intensity of the oxidation current accompanies an increase in the scanning rate. If this dependence is presented as a ratio of the obtained current for each value of the square root of the scan rate, a linear curve is obtained that can be represented by the following equation: $y = 0.590x - 0.823$ (Figure 4B). The correlation coefficient is $R^2 = 0.9921$. This linearity is a confirmation that the diffusion-controlled process represents the nature of the electrode reaction on the electrode surface. In addition, one can notice that there is also a slight shift of peak oxidation towards higher values of the potential with increasing scan rate. This phenomenon, however, is a feature of the adsorption-controlled process at high scanning speeds. This claim can be confirmed by the appearance of the voltammograms themselves at higher scanning speeds. This is a general feature of this system and has been reported by other authors as well [27,38]. Furthermore, the logarithmic relationship between the oxidation peak current and scan rate was analyzed and it is presented in Figure 4C. The linear dependence is represented by the equation $y = 0.592x - 0.489$ ($R^2 = 0.9983$), with a slope very close to the theoretical value for diffusion-controlled processes (0.5), which indicates a dominantly diffusion-controlled process, with a possible slight contribution of adsorption. This phenomenon can be confirmed with negligible peak shifts at higher scan rate values.

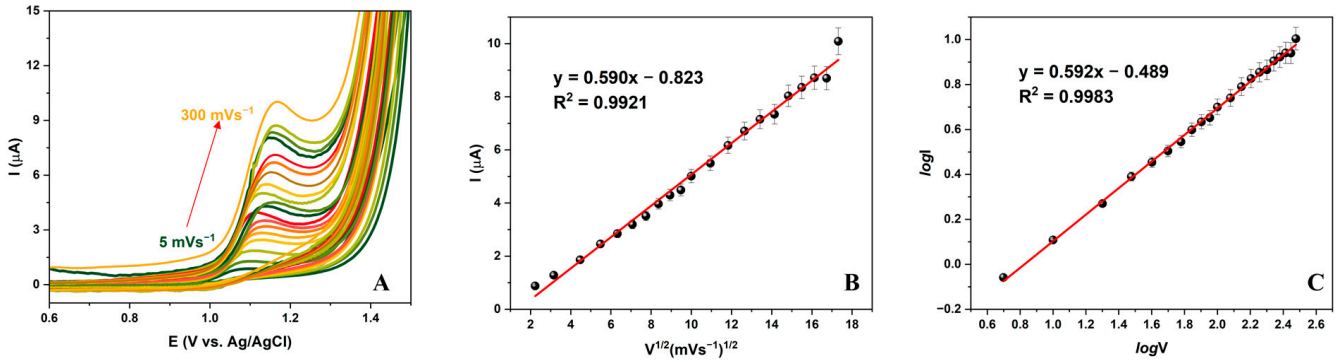


**Figure 4.** (**A**) Cyclic voltammograms of 100 μM QN using 5% BiOCl-modified CPE in BRBS at pH 6 at different scan rates in the range from 2 to 200 $mVs^{-1}$; (**B**) Dependence of redox peak current on the square root of scan rate; (**C**) The linear logarithmic relationship between oxidation peak current and scan rate.

### *3.4. Quantification of QN*

Employing techniques that enhance the ratio of faradaic to capacitive current and consequently raise the detection sensitivity allows for quantitative analysis in voltammetry. Square-wave voltammetry (SWV) and differential pulse voltammetry (DPV) are the techniques most frequently employed for this purpose. Differential pulse voltammetry was selected for the quantitative determination of QN after these two approaches were compared because it produced a better signal at the QN oxidation potential (Figure S1).

DPV measurements were recorded at amplitude 25 mV with both pulse width and period 0.2 s, in a potential range from 0.6 to 1.5 V. Good results in improving the properties of the carbon paste electrode were validated by utilizing previously optimized working parameters to analyze the effects of different concentrations of analyte. Figure 5A represents the voltammetric response of the developed sensor over different concentrations of QN in the range from 10 µM to 140 µM, where linear dependence was obtained. Noticeable peak shifts at higher concentrations confirm a slight contribution of the adsorption of the analyte at the electrode surface. Figure 5B illustrates how the oxidation current is affected by the addition of a standard QN solution. The calibration curve is described by the equation $y = 0.014x + 0.273$ with a linear regression coefficient of 0.9745. Based on the values of the calibration curve's slope and the blank's standard deviation, the limits of detection (LOD) and quantification (LOQ) were determined using the following relations: LOD is $3\sigma/S$ and LOQ is $10\sigma/S$. In addition, the sensitivity of the developed sensor was calculated as S/A, where A stands for the surface area of the electrode. The values of these parameters were acquired: LOD = 0.14 µM, LOQ = 0.47 µM, and sensitivity = 1.995 µA $\mu M^{-1}$ $cm^{-2}$.

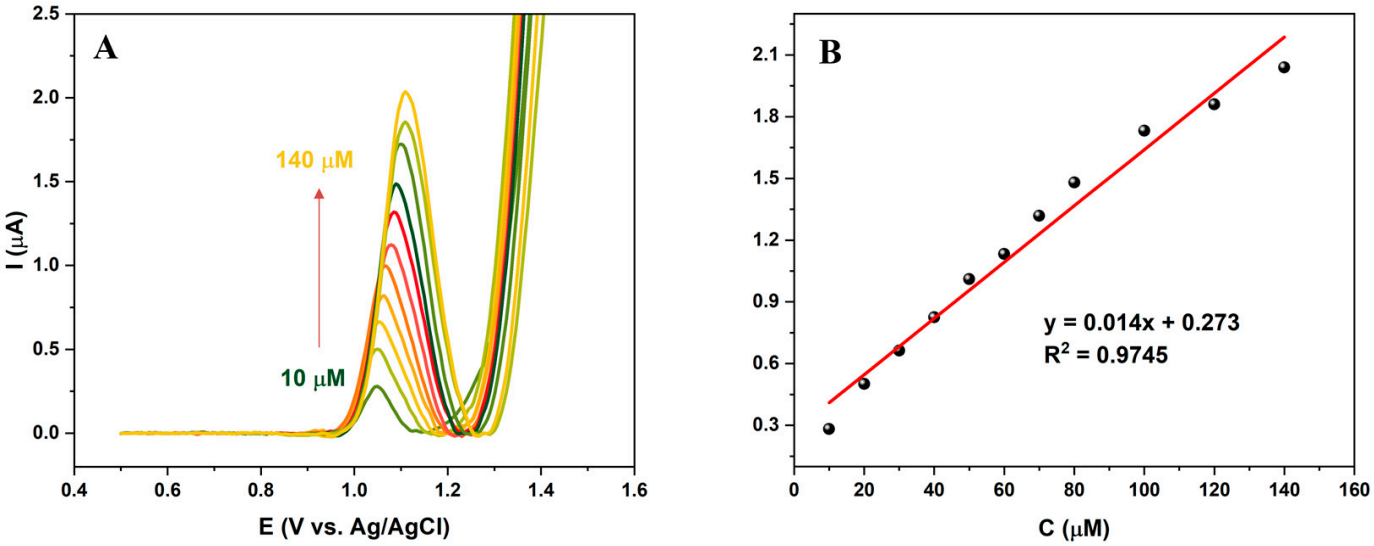


**Figure 5.** (**A**) The DPV voltammetric response over the 5% BiOCl-modified CPE toward various concentrations of QN (10–140 µM) in a potential range from 0.5 to 1.4 V at amplitude 25 mV and pulse width and period of 0.2 s; (**B**) Calibration curve of QN for the concentration range from 10 to 140 µM.

In summary, our findings were compared with those of other modified electrodes by looking at the method's most crucial analytical parameters, like linear range and detection limit, as well as how the method was applied to actual samples. Our results are comparable in terms of operating range and detection limit (Table 1). The most significant benefit of our sensor is the ease of material preparation, environmentally friendly synthesis, and a wider linear range of operation. Additionally, according to the World Health Organization [40], QN exhibits toxic effects on humans in concentrations higher than 100 mg/L (or 308.25 µM), and it is not present in medicines and beverages in concentrations higher than 166 mg and

85 mg/L, respectively. In conclusion, the developed sensor with its properties can be easily applied to analyze various real samples such as pharmaceuticals and food and beverage samples.

**Table 1.** Comparison between recently reported results for QN detection.

| Electrode | Method | pH | LR (μM) | LOD (μM) | Sample | Ref. |
|---|---|---|---|---|---|---|
| BDDE | DPV | 5.5 | 0.1–1.96 | 0.07 | soft drinks and urine | [30] |
| p-(AHNSA)/GCE | SWV | 7 | 0.1–100 | 0.0142 | urine and pharmaceutical formulations | [38] |
| MIP–MIC-AuNPs/MWCNT-chitosan/PGE | DPV | 8 | $10^{-7}$–$10^{-3}$ | $5 \times 10^{-8}$ | blood and urine | [28] |
| MWCNTs-RTIL/GCE | SWV | 6.8 | 3–100 | 0.44 | commercial injection | [39] |
| HMDE | SWV | 10.4 | 9.73–74.62 | 0.043 | soft drinks | [6] |
| BiOCl/CPE | DPV | 6 | 10–140 | 0.14 | soft drinks | This work |

### *3.5. Stability, Repeatability, and Reproducibility Studies*

For this part, the goal was to examine the response of one electrode during the recording of the same concentration of quinine over a day, as well as to examine the response of several different electrodes to the same concentration of quinine. This would provide data on the reproducibility and repeatability of measurements. For both of these measurements (20 μM quinine), the relative standard deviation values obtained were less than 5%. This result indicates that the proposed sensor is adequately reproducible and that the reproducibility of the measurements is also very high. Additionally, measurement stability was monitored throughout the study, using prepared paste. A concentration of 20 μM quinine was measured every 3 days. In the meantime, the electrode stood in ambient conditions, protected from light. After 45 days of monitoring, the ratio initial peak/recorded peaks were at a value of 5.7%. If it is taken into account that the proposed sensor, like other CPE electrodes, is a homemade heterogeneous structure, it can be considered that the obtained deviation values do not represent a significant deviation and that the developed method and the prepared sensor can be tested in work with real samples.

### *3.6. Selectivity Studies*

The selectivity of the sensor is one of the most important parameters during method development. To evaluate the selectivity of the BiOCl@CPE sensor for QN detection, different metal and organic compound solutions were examined. DPV measurements were performed under optimized parameters in 100 μM QN solution with the addition of 100 μM interference solutions (1:1 $v/v$). Our findings revealed that the presence of metals (Ca, K, Cu, Mg, Na), ascorbic acid (AA), glucose (Glu), uric acid (UA), levofloxacin (LEV), and paracetamol (PAR) did not interfere with the quantification of QN, resulting in changes in the current signal of less than 3% (Figure S2).

### *3.7. Real Sample Analysis*

The developed method was used for the determination of QN in beverages. A tonic drink that has no more than 85 mg/L according to the declaration was tested, after 2 preparation steps: ultrasonic degassed for 7 minutes and dilution 2.5 times with BRBS pH 6. DPV measurements were performed under optimized parameters with a 5% BiOCl-modified electrode. The measurement was repeated in triplicate and the relative standard deviation

of the measurement was 4.3%, which fully fits the previously obtained values of the repeatability of the method. These results support the fact that the influence of the matrix is negligible and that the developed sensor system is highly selective for the determination of quinones in real samples. Using a calibration curve and UV–Vis validation, the concentration of QN in a tonic water beverage was determined. Figure 6A represents the DPV voltammogram of the drink sample. The diluted sample gave an oxidation peak on 1.1 V potential with a peak current of 0.8605 µA, and the calculated value of QN concentration in tonic drink is 59.51 mg/L. Figure 6B shows the UV–Vis Spectra of 5, 15, 25, 35, and 45 mg/L QN standard solutions and the sample solution prepared in the same way. After plotting the calibration curve, the sample gave an absorbance value of 0.3976, and QN concentration was determined from equation y = 0.016x + 0.003. QN concentration obtained by UV–Vis is 60.58 mg/L, which follows previously obtained results using the developed sensor and the declaration of the drink. Considering all the above, the developed sensor can be utilized as a new method for QN determination in beverage samples.

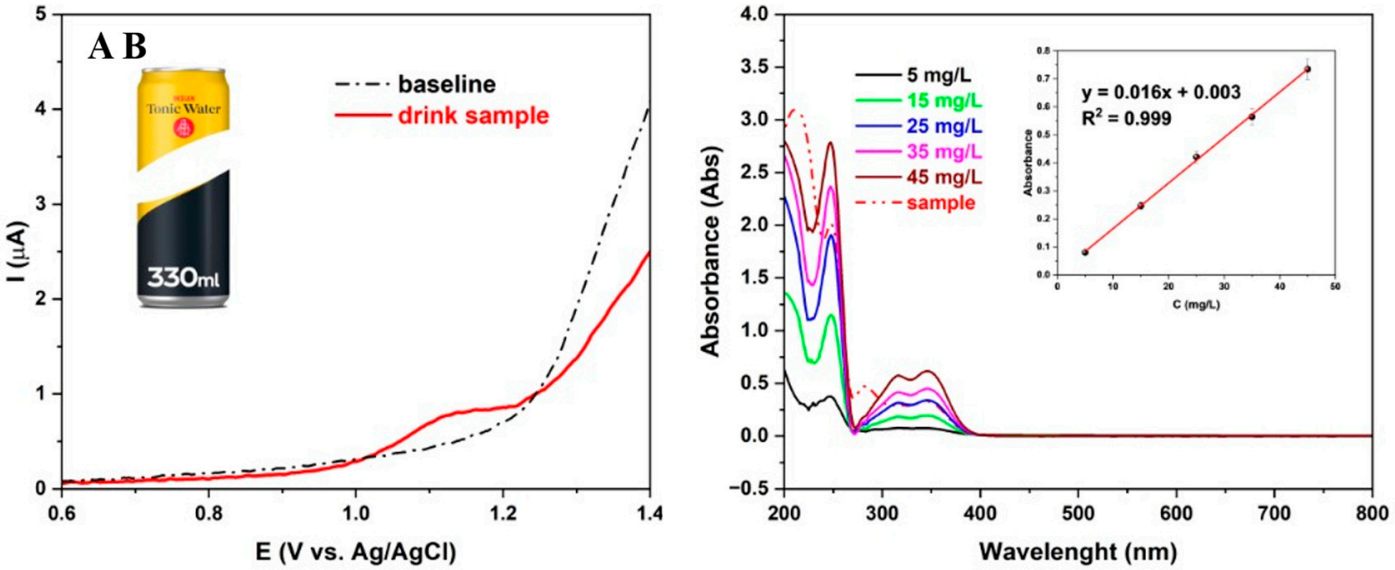


**Figure 6.** Determination of QN in beverage sample using (**A**) The developed sensor; (**B**) The standard UV–Vis method, with the inserted image representing the corresponding calibration curve.

## 4. Conclusions

To summarize, we have successfully applied an organic solvent-free hydrothermal method to synthesize highly crystalline pseudospherical BiOCl nanoparticles. Using TEM, SEM, and XRD techniques, we carefully assessed the nanomaterial's morphological properties. The electrochemical performance of a BiOCl-supported carbon paste electrode for QN detection showed rapid electron transfer kinetics, with remarkable electroactivity. The developed detection method, DPV, under optimized working conditions exhibited excellent stability, repeatability, and reproducibility over a wide linear range (10–140 µM), low detection limit (0.14 µM), and high sensitivity (1.995 µA $\mu M^{-1}$ $cm^{-2}$). Additionally, the BiOCl@CPE sensor demonstrated practical applicability in beverage samples, which was validated using the standard UV–Vis method. In conclusion, the developed BiOCl@CPE sensor presents a promising material for the effective electrochemical detection of QN, with potential applications in beverage sample analysis. This method can be easily applied in routine research by using the standard addition method or a calibration curve.

**Supplementary Materials:** The following supporting information can be downloaded at: https://www.mdpi.com/article/10.3390/electrochem5040027/s1, Figure S1: (**A**) Comparison between DPV and SWV methods for QN quantification with corresponding bar graph (**B**); Figure S2: Bar graph of the peak currents of QN without and with the addition of potential interfering species.

**Author Contributions:** Conceptualization, V.S., N.S. and D.S.; methodology, T.M. and G.G.; formal analysis, T.M., V.B.N. and M.O.; investigation, T.M. and G.G.; writing—original draft preparation, T.M., V.S., M.O. and D.S.; supervision N.S. and D.S. All authors have read and agreed to the published version of the manuscript.

**Funding:** This research received no external funding.

**Institutional Review Board Statement:** Not applicable.

**Informed Consent Statement:** Not applicable.

**Data Availability Statement:** Data are contained within the article.

**Acknowledgments:** This work was financially supported by the Ministry of Science, Technological Development, and Innovation of the Republic of Serbia, contract nos.: 451-03-66/2024-03/200168 and 451-03-66/2024-03/200026.

**Conflicts of Interest:** The authors declare no conflicts of interest.

## References

1. World Health Organization. World Malaria Report 2022. Available online: https://www.who.int/teams/global-malaria-programme (accessed on 1 September 2024).
2. Leoriza, M.D.; Sabriena, N.; Ramadhan, M.R.; Tajalla, G.U.N.; Umaningrum, D.; Ismail, A.I.; Ogata, G.; Einaga, Y.; Triana, Y. Study of Quinine Hydrochloride Detection Using Boron-Doped Diamond Electrodes. *Int. J. Electrochem. Sci.* **2024**, *19*, 100778. [CrossRef]
3. Gong, H.; Bao, C.; Luo, X.; Yu, Y.; Yang, W. Reusable electrochemical sensor for quinine detection via β-cyclodextrin-based indicator displacement assay. *Microchem. J.* **2024**, *198*, 110109. [CrossRef]
4. Nate, Z.; Gill, A.A.; Chauhan, R.; Karpoormath, R. Recent progress in electrochemical sensors for detection and quantification of malaria. *Anal. Biochem.* **2022**, *643*, 114592. [CrossRef] [PubMed]
5. Sato, S. Plasmodium—A brief introduction to the parasites causing human malaria and their basic biology. *J. Physiol. Anthr.* **2021**, *40*, 1–13. [CrossRef] [PubMed]
6. Dar, R.A.; Brahman, P.K.; Tiwari, S.; Pitre, K.S. Electrochemical studies of quinine in surfactant media using hanging mercury drop electrode: A cyclic voltammetric study. *Colloids Surf. B Biointerfaces* **2012**, *98*, 72–79. [CrossRef]
7. Bannon, P.; Yu, P.; Cook, J.M.; Roy, L.; Villeneuve, J.-P. Identification of quinine metabolites in urine after oral dosing in humans. *J. Chromatogr. B Biomed. Sci. Appl.* **1998**, *715*, 387–393. [CrossRef]
8. Donovan, J.L.; DeVane, C.; Boulton, D.; Dodd, S.; Markowitz, J.S. Dietary levels of quinine in tonic water do not inhibit CYP2D6 in vivo. *Food Chem. Toxicol.* **2003**, *41*, 1199–1201. [CrossRef]
9. Shrivas, K.; Wu, H.-F. Quantitative bioanalysis of quinine by atmospheric pressure-matrix assisted laser desorption/ionization mass spectrometry combined with dynamic drop-to-drop solvent microextraction. *Anal. Chim. Acta* **2007**, *605*, 153–158. [CrossRef]
10. Imanzadeh, H.; Sefid-Sefidehkhan, Y.; Afshary, H.; Afruz, A.; Amiri, M. Nanomaterial-based electrochemical sensors for detection of amino acids. *J. Pharm. Biomed. Anal.* **2023**, *230*, 115390. [CrossRef]
11. Maduraiveeran, G.; Jin, W. Nanomaterials based electrochemical sensor and biosensor platforms for environmental applications. *Trends Environ. Anal. Chem.* **2017**, *13*, 10–23. [CrossRef]
12. Curulli, A. Nanomaterials in Electrochemical Sensing Area: Applications and Challenges in Food Analysis. *Molecules* **2020**, *25*, 5759. [CrossRef] [PubMed]
13. Ognjanović, M.; Nikolić, K.; Radenković, M.; Lolić, A.; Stanković, D.; Živković, S. Picosecond laser-assisted synthesis of silver nanoparticles with high practical application as electroanalytical sensor. *Surf. Interfaces* **2022**, *35*, 102464. [CrossRef]
14. Đurđić, S.; Vlahović, F.; Ognjanović, M.; Gemeiner, P.; Sarakhman, O.; Stanković, V.; Mutić, J.; Stanković, D.; Švorc, Ľ. Nano-size cobalt-doped cerium oxide particles embedded into graphitic carbon nitride for enhanced electrochemical sensing of insecticide fenitrothion in environmental samples: An experimental study with the theoretical elucidation of redox events. *Sci. Total. Environ.* **2024**, *909*, 168483. [CrossRef] [PubMed]
15. Martynov, L.Y.; Sadova, M.K.; Sakharov, K.A.; Yashtulov, N.A.; Zaytsev, N.K. Determination of indium by adsorptive stripping voltammetry at the bismuth film electrode using combined electrode system facilitating medium exchange. *Talanta* **2024**, *271*, 125680. [CrossRef] [PubMed]

16. De Benedetto, A.; Della Torre, A.; Guascito, M.R.; Di Corato, R.; Chirivì, L.; Rinaldi, R.; Aloisi, A. Spectroscopic investigations of a commercial graphite screen printed electrode modified by bismuth oxide drop deposition and electrochemical reduction, for cadmium and lead ions simultaneous determination. *J. Electroanal. Chem.* **2024**, *964*. [CrossRef]
17. Bi, H.; Zhang, W.; Cao, P. Effect of bismuth doping on electrodeposition, physicochemical properties and electrocatalytic activity of lead dioxide electrodes. *Int. J. Electrochem. Sci.* **2024**, *19*, 100635. [CrossRef]
18. Chmurzyński, L. High-performance liquid chromatographic determination of quinine in rat biological fluids. *J. Chromatogr. B: Biomed. Sci. Appl.* **1997**, *693*, 423–429. [CrossRef]
19. Samanidou, V.F.; Evaggelopoulou, E.N.; Papadoyannis, I.N. Simultaneous determination of quinine and chloroquine anti-malarial agents in pharmaceuticals and biological fluids by HPLC and fluorescence detection. *J. Pharm. Biomed. Anal.* **2005**, *38*, 21–28. [CrossRef]
20. Li, B. Flow-injection chemiluminescence determination of quinine using on-line electrogenerated cobalt(III) as oxidant. *Talanta* **2000**, *51*, 515–521. [CrossRef]
21. Zhang, W.; Danielson, N.D. Determination of phenols by flow injection and liquid chromatography with on-line quinine-sensitized photo-oxidation and quenched luminol chemiluminescence detection. *Anal. Chim. Acta* **2003**, *493*, 167–177. [CrossRef]
22. Damien, R.; Daval, S.; Souweine, B.; Deteix, P.; Eschalier, A.; Coudoré, F. Rapid gas chromatography/mass spectrometry quinine determination in plasma after automated solid-phase extraction. *Rapid Commun. Mass Spectrom.* **2006**, *20*, 2528–2532. [CrossRef] [PubMed]
23. Jain, R.; Mudiam, M.K.R.; Ch, R.; Chauhan, A.; A Khan, H.; Murthy, R. Ultrasound Assisted Dispersive Liquid–Liquid Microextraction Followed by Injector Port Silylation: A Novel Method for Rapid Determination of Quinine in Urine by GC–MS. *Bioanalysis* **2013**, *5*, 2277–2286. [CrossRef] [PubMed]
24. Kluska, M.; Marciniuk-Kluska, A.; Prukała, D.; Prukała, W. Determination of Quinine, Quinidine, and Cinquinidine by Capillary Electrophoresis. *J. Liq. Chromatogr. Relat. Technol.* **2015**, *38*, 886–890. [CrossRef]
25. Mikuš, P.; Maráková, K.; Veizerová, L.; Piešťanský, J. Determination of quinine in beverages by online coupling capillary isotachophoresis to capillary zone electrophoresis with UV spectrophotometric detection. *J. Sep. Sci.* **2011**, *34*, 3392–3398. [CrossRef] [PubMed]
26. Mutić, T.; Ognjanović, M.; Kodranov, I.; Robić, M.; Savić, S.; Krehula, S.; Stanković, D.M. The influence of bismuth participation on the morphological and electrochemical characteristics of gallium oxide for the detection of adrenaline. *Anal. Bioanal. Chem.* **2023**, *415*, 4445–4458. [CrossRef]
27. Sochr, J.; Švorc, Ľ.; Rievaj, M.; Bustin, D. Electrochemical determination of adrenaline in human urine using a boron-doped diamond film electrode. *Diam. Relat. Mater.* **2014**, *43*, 5–11. [CrossRef]
28. Azadmehr, F.; Zarei, K. Fabrication of an imprinted electrochemical sensor from l-tyrosine, 3-methyl-4-nitrophenol and gold nanoparticles for quinine determination. *Bioelectrochemistry* **2019**, *127*, 59–67. [CrossRef]
29. Buleandra, M.; Rabinca, A.A.; Cheregi, M.C.; Ciucu, A.A. Rapid voltammetric method for quinine determination in soft drinks. *Food Chem.* **2018**, *253*, 1–4. [CrossRef]
30. Dushna, O.; Dubenska, L.; Marton, M.; Hatala, M.; Vojs, M. Sensitive and selective voltammetric method for determination of quinoline alkaloid, quinine in soft drinks and urine by applying a boron-doped diamond electrode. *Microchem. J.* **2023**, *191*, 108839. [CrossRef]
31. Kaleeswarran, P.; Priya, T.S.; Chen, T.-W.; Chen, S.-M.; Kokulnathan, T.; Arumugam, A. Construction of a Copper Bismuthate/Graphene Nanocomposite for Electrochemical Detection of Catechol. *Langmuir* **2022**, *38*, 10162–10172. [CrossRef]
32. Zhang, X.; Ai, Z.; Jia, F.; Zhang, L. Generalized One-Pot Synthesis, Characterization, and Photocatalytic Activity of Hierarchical BiOX (X = Cl, Br, I) Nanoplate Microspheres. *J. Phys. Chem. C* **2008**, *112*, 747–753. [CrossRef]
33. Li, T.; Liu, T.; Wei, H.; Gu, X. Facile synthesis of different 3D bismuth oxychloride hierarchitectures and their visible-light photocatalytic properties. *J. Mater. Sci. Mater. Electron.* **2016**, *27*, 3456–3461. [CrossRef]
34. Laschuk, N.O.; Easton, E.B.; Zenkina, O.V. Reducing the resistance for the use of electrochemical impedance spectroscopy analysis in materials chemistry. *RSC Adv.* **2021**, *11*, 27925–27936. [CrossRef] [PubMed]
35. Zhu, P.; Zhao, Y. Cyclic voltammetry measurements of electroactive surface area of porous nickel: Peak current and peak charge methods and diffusion layer effect. *Mater. Chem. Phys.* **2019**, *233*, 60–67. [CrossRef]
36. Venkatesh, K.; Muthukutty, B.; Chen, S.-M.; Karuppasamy, P.; Haidyrah, A.S.; Karuppiah, C.; Yang, C.-C.; Ramaraj, S.K. Spinel CoMn2O4 nano-/micro-spheres embedded RGO nanosheets modified disposable electrode for the highly sensitive electrochemical detection of metol. *J. Ind. Eng. Chem.* **2022**, *106*, 287–296. [CrossRef]
37. Mutić, T.; Stanković, D.; Manojlović, D.; Petrić, D.; Pastor, F.; Avdin, V.V.; Ognjanović, M.; Stanković, V. Micromolar Levofloxacin Sensor by Incorporating Highly Crystalline $Co_3O_4$ into a Carbon Paste Electrode Structure. *Electrochem* **2024**, *5*, 45–56. [CrossRef]
38. Geto, A.; Amare, M.; Tessema, M.; Admassie, S. Polymer-modified glassy carbon electrode for the electrochemical detection of quinine in human urine and pharmaceutical formulations. *Anal. Bioanal. Chem.* **2012**, *404*, 525–530. [CrossRef]

39. Zhan, X.-M.; Liu, L.-H.; Gao, Z.-N. Electrocatalytic oxidation of quinine sulfate at a multiwall carbon nanotubes-ionic liquid modified glassy carbon electrode and its electrochemical determination. *J. Solid State Electrochem.* **2011**, *15*, 1185–1192. [CrossRef]
40. Food and Agriculture Organization; World Health Organization. *Evaluation of Certain Food Additives and Contaminants: Forty-First Report of the Joint FAO/WHO Expert Committee on Food Additives*; WHO Press: Geneva, Switzerland, 1993; WHO Library Cataloguing-in-Publication Data. WHO Technical Report Series; no. 837; ISBN 92-4-120837-6. Available online: https://www.who.int/publications/i/item/9241208376 (accessed on 1 September 2024).